INFORMATION REPORT INFORMATION REPORT

CENTRAL INTELLIGENCE AGENCY

~~SECRET~~

COUNTRY East Germany

SUBJECT Reports on Antenna Testing and Phase Testing Sites

REPORT

DATE DISTR. 23 AUG 1962

NO. PAGES 38

REFERENCES RD

50X1-HUM

50X1-HUM

50X1-HUM

DATE OF INFO.

PLACE & DATE ACQ.

50X1-HUM

50X1-HUM

THIS IS UNEVALUATED INFORMATION. SOURCE GRADINGS ARE DEFINITIVE. APPRAISAL OF CONTENT IS TENTATIVE.

50X1-HUM

50X1-HUM

5 4 3 2 1

~~SECRET~~

GROUP 1
EXCLUDED FROM AUTOMATIC DOWNGRADING AND DECLASSIFICATION

STATE	ARMY	NAVY	AIR	NSA		DIA	AID
X	X	X	X	X		X	

OSI EV X

(Note: Washington distribution indicated by "X"; Field distribution by "#".)

INFORMATION REPORT INFORMATION REPORT

178

S-E-C-R-E-T

REPORT

COUNTRY : East Germany

DATE DISTR. 27 Jul 62

SUBJECT : Reports on Antenna Testing and Phase Testing Sites

NO. OF PAGES 37

DATE OF INFORMATION:

REFERENCES:

PLACE ACQUIRED :

THIS IS UNEVALUATED INFORMATION

S-E-C-R-E-T

50X1-HUM

Introduction.

On 20 March 1961, the Radio Mechanics Plant (VEB Entwicklungswerk Funkmechanik), Leipzig-Plagwitz, sent a report of its phase-measuring grounds for microwave antennas to the Koppenick Radio Plant (VEB Funkwerk Koepenick).

A translation of the report follows.

50X1-HUM

Reports on Antenna Testing and Phase-Testing Sites

50X1-HUM

the technical report on phase testing site is enclosed.

50X1-HUM

On the basis of the work conducted at the testing station and the continued improvement, these reports, naturally, no longer correspond to the newest developments, but they are still the most important reports available.

50X1-HUM

Table of Contents

9. Evaluation of Test Results.

10. Operating Instructions.

11. Summary.

12. Bibliography.

Technical Report

Phase Testing Station for Microwave Antennas, Especially for Determining the Radiation Center of the Primary Emitter

by Jochen Alter

1. Purpose of the Phase Testing Station.

In building a mirror or lens antenna, the most heterogeneous types of active emitters are used. One thing is common to all, however: that they do not have a punctiform source of radiation. On the other hand, however, a parabola or a cylindrical parabola has the characteristic of a focal point or focal line. Optimum reflection conditions are obtained only when the radiation source is a point or a line source exactly in the focusing point or focal line. If we are far enough away from an emitter of an arbitrary geometrical form, we can demonstrate that the areas of the same phase of the electromagnetic radiation field are spherical. If that is so, however, a mid-point of the sphere can be determined backwards and designated as the radiation mid-point or radiation center. It seems significant to place the center in the focusing point. Actually, maximum gain is obtained from a parabolic antenna when the radiation center of the primary emitter is in the focusing point of the parabola. If the position of the center is not known, a certain amount of defocusing has to be done, which usually causes undesirable changes in the entire radiation diagram.

The problem is especially interesting when, for example, a horn emitter is used as a radiation source and the entire antenna is to be used not only for one frequency but for a larger frequency band. It is then possible to determine the radiation center with one of the frequency-dependent shifts. It may already be known theoretically[1] that with increasing frequency the center of radiation shifts from the surface of the aperture toward the inside of the emitter if it is a horn emitter with a definite aperture angle. It is thus possible to determine the area in which the center of radiation moves.

The reason for the existence of the phase testing station is to make it possible to determine the radiation center of any active (primary) emitter by technical measurements. Another possibility of its use is to record the phase diagram. This shows the relationship of the phase of the radiation field to the angle as measured toward the emitter axis. This causes phase angle shifts in the E as well as the H plane, at least theoretically, between, for example, the direction of the main beam and the direction of a secondary beam. In practice we do not find a break there, but rather a continuous transition from 0 to 180 degrees. A facility such as this is described in reference 2.

2. The Theory of Testing the Radiation Center.

Figure 1

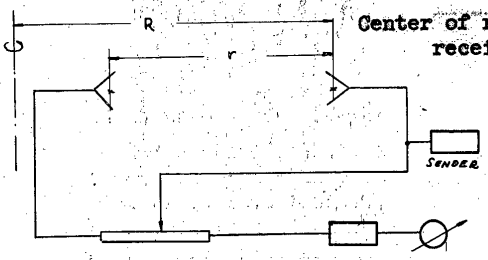

The measurement is based on a phase comparison between the voltage that passes over the antenna field and the sonde, which is transmitted to the instrument leads.[3] If both amplitudes are the same and the phases are displaced by (illegible), the receiver does not get any voltage and the indicating instrument remains on zero. If distance, r, is changed, a new matching position, x, is to be looked for on the instrument lead. In Figure 1 it is indicated that r is measured between the radiation center of both antennas, the positions of which are considered known. If the receiving antenna is rotated on a pivot by a definite angle, ψ, the phase over the range of measurement does not remain constant because r increases (Figure 2). This difference, d, is determined on the instrument lead and, with ψ, represents a unit for the distance of the radiation center, Z_E, from the axis of rotation.

Figure 2

1. Axis of rotation.
2. Phase front.

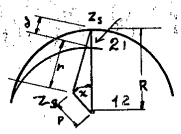

If we make $\varphi = R-r = 0$, that is, Z_E and the axis of rotation coincide, a phase change on the basis of turning the receiving antenna is not be be expected as long as the phase remains constant in a dial sector, for example, within the main beam direction of the receiver antenna. If ψ is further increased, then secondary rays are attained in the transition area. The phase is then displaced by (illegible) without r having changed. In this an important assumption is to be recognized: The measurement may be conducted only within a dial sector in which the phase is equal. Border areas are to be avoided because the transition to secondary radiation does not occur suddenly. Under certain circumstances, the radiation diagram is to be consulted.

(One paragraph of the original here was illegible.)

From this it may be assumed that $r \geq 2 \frac{D^2}{\lambda_o}$ (2.1)

is to be expected in every case. This means that D is the greatest dimension of a radiating antenna (diagonal to the aperture surface, diameter of the aperture surface, length of one of the dipoles, etc.). The wavelength, λ_o, is that existing in free space.

Figure 2 should be consulted when calculating ϱ.

If we use the law of cosines on the triangle with the sides R, ϱ, and r + d, then

$$(r + d)^2 = R^2 + \varrho^2 - 2R\varrho\cos\psi$$

is obtained, and, in this case, ϱ = R-r may be calculated as

$$\varrho = \frac{d\left(1 + \frac{1}{2}\frac{d}{R}\right)}{1 - \cos\psi\cdot\frac{d}{R}} \qquad (2.2)$$

Since d/R << 1 (d has the order of magnitude of millimeters and R, on the other hand, of meters), the following approximation is sufficient:

$$\varrho = \frac{d}{1 - \cos\psi + \frac{d}{R}} \qquad \varrho = \frac{d}{2\sin^2\frac{\psi}{2} + \frac{d}{R}} \qquad (2.3)$$

If the point of rotation is between the two radiation centers, it may then be calculated analogously that

$$\varrho = \frac{d\left(1 - \frac{1}{2}\frac{d}{R}\right)}{1 - \cos\psi - \frac{d}{R}} \qquad (2.4)$$

or for $\frac{d}{R} << 1$

$$\varrho = \frac{d}{1 - \cos\psi\,\frac{d}{R}} \qquad \varrho = \frac{d}{2\sin^2\psi_{/2} - \frac{d}{R}} \qquad (2.5)$$

The minus sign appeared, therefore, because in an arrangement such as this the distances r and d are shortened by swinging the receiver antenna around ψ.

Equation 2.3 should be further discussed here because the testing station is built up as indicated in Figure 1.

3. Testing and Evaluation Methods.

According to the product (Equation 2.3), it is therefore sufficient to rotate the receiver antenna, which, at the same time, represents the one to be investigated, around angle ψ toward the connecting-line point of rotation, $-Z_S$, to measure the proper displacement of the equalizing point on instrument lead d, in order to obtain the desired distance of the point of rotation, $-Z_E$, that is, R-r = ϱ.

The problem dealing with error is of unusual interest: the absolute error, $\Delta\varrho$, by which the result may vary on the basis of an error in measuring ψ, d, and R. For the sake of simplicity, we presuppose that the errors $\Delta\psi$, Δd, and ΔR are very small in comparison to their absolute magnitude and for that reason can set the complete differential $d\varrho \approx \Delta\varrho$ as follows:

$$\Delta\varrho = \frac{\delta\varrho}{\delta d}\,\Delta d + \frac{\delta\varrho}{\delta\psi}\,\Delta\psi + \frac{\delta\varrho}{\delta R}\,\Delta R \qquad (3.1)$$

In particular, with Equation 2.3, the following is obtained:

$$\frac{\delta\varrho}{\delta d} = \frac{2\sin^2\frac{\psi}{2} + \frac{d}{R} - \frac{d}{R}}{\left(2\sin^2\frac{\psi}{2} + \frac{d}{R}\right)^2} = \frac{2\sin^2\frac{\psi}{2}}{\left(2\sin^2\frac{\psi}{2} + \frac{d}{R}\right)^2} = F_1 \qquad (3.2)$$

$$\frac{\delta\varrho}{\delta\psi} = \frac{-d\,2\sin\frac{\psi}{2}\cdot\cos\frac{\psi}{2}}{\left(2\sin^2\frac{\psi}{2} + \frac{d}{R}\right)^2} = \frac{-d\sin\psi}{\left(2\sin^2\frac{\psi}{2} + \frac{d}{R}\right)^2} = F_2\,d \qquad (3.3)$$

$$\frac{\delta\varrho}{\delta R} = \frac{\left(\frac{d}{R}\right)^2}{\left(2\sin^2\frac{\psi}{2} + \frac{d}{R}\right)^2} = F_3 \qquad (3.4)$$

The error $\Delta\varphi$ can, therefore, be represented by three error functions, F_1, F_2, and F_3, which describe each influence of Δd, $\Delta\psi$, and ΔR, as follows:

$$\Delta\varphi = F \cdot \Delta d - F_2\, d\, \Delta\psi + F_3\, \Delta R \qquad (3.5)$$

Diagram 1 includes the three error functions as a function of ψ and d/R as the parameter. From this it may be seen that a measurement below ψ = 8° to 10° will cause very great errors. Therefore, an evaluation only above that angle is recommended. The greatest contribution is made by the angle error; therefore d cannot be too large. This means that the point of rotation, Z_E, should not be set at too large a distance. Naturally, it should be large enough to allow sensible displacements, d, to be read on the instrument lead ($\approx$ 10 mm). It is satisfactory, however, when this d is reached in connection with $\psi > 6°$.

The solution with Equation 2.3 presupposes that with ψ = 0, Z_S is kept on a line with the actual point of rotation, Z_E. This cannot always be the case because of assembly errors, especially since the exact position of Z_E is not known. Small dissymmetries of the emitter are sufficient to prevent the geometrical and electrical axes from coinciding.

If we consider the function $X(\psi)$ in which x represents the place of asymmetry on the instrument lead, we obtain, for example, a diagram like Figure 3. It is therefore foolish to start with ψ = 0. Rather we should start with $X(\psi)$, determine ψ_c, and then begin the evaluation. Since the determination of ψ_c, however, depends on the reliable determination of the maximum of curve $X(\psi)$, it is probably desirable to be able to calculate the difference Δd and $\Delta\psi = \psi_2 - \psi_1$.

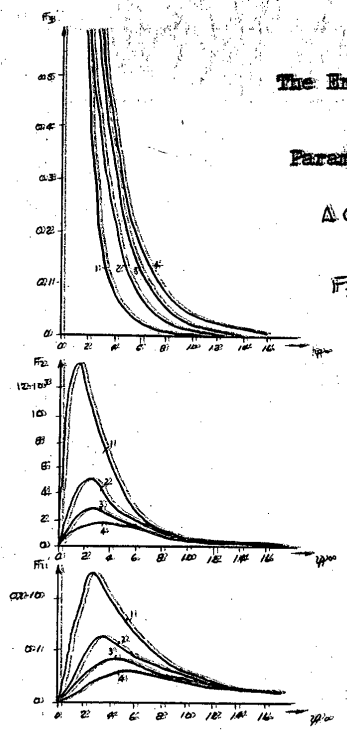

Diagram 1

The Error Function as a Function of ψ.

Parameter: $\frac{d}{R} = 1 \cdot 10^{-3}, 2 \cdot 10^{-3}, 3 \cdot 10^{-3}, 4 \cdot 10^{-3}$

$$\Delta\varphi = F_1\, \Delta d - F_2 \cdot d \cdot \Delta\psi + F_3 \Delta R$$

$$F_3 = \frac{\left(\frac{d}{R}\right)^2}{\left(2\sin^2\frac{\psi}{2} + \frac{d}{R}\right)^2}$$

$$F_2 = \frac{\sin\psi}{\left(2\sin^2\frac{\psi}{2} + \frac{d}{R}\right)^2}$$

$$F_1 = \frac{2\sin^2\frac{\psi}{2}}{\left(2\sin^2\frac{\psi}{2} + \frac{d}{R}\right)^2}$$

Figure 3

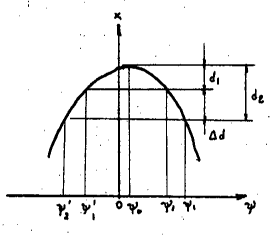

This desire is only partly realizable because, in order to determine the angle, a point of departure or reference point is certainly needed. But this method does have an advantage, in that Δd can be determined with a smaller error than d, because even the height of the maximum cannot be read so well.

Let us now briefly derive for Δd and ψ_1, ψ_2 the equation for φ. Therefore, with Equation 2.3, $d_2 = d_1 + \Delta d$ is expressed as follows:

$$\varphi = \frac{d_1 + \Delta d}{2 \sin^2 \frac{\psi_2}{2} + \frac{d_1 + \Delta d}{R}} \qquad (3.5a)$$

If we convert Equation 2.3 for ψ_1 and d_1, after d_1 we obtain

$$d_1 = \frac{R}{r} \varphi \, 2 \sin^2 \frac{\psi_1}{2} \qquad (3.5b)$$

If d_1 is included in the upper equation, 3.5a, then we obtain

$$\varphi = \frac{\Delta d}{2\left(\sin^2 \frac{\psi_1}{2} - \sin^2 \frac{\psi_1}{2}\right) + \frac{\Delta d}{R}} \qquad (3.6)$$

As we can see, Equation 2.3 could also have been interpreted as a special application of Equation 3.6 with $\psi_1 = 0$; then again instead of obtaining only d_2 we get Δd.

The evaluation process now proceeds as follows: Either Figure 3 is evaluated as indicated, i.e., determine ψ_1 and ψ_2 corresponding to ψ_1 and ψ_2, and obtain the real angle which is to be inserted in Equation 3.6 from

$$\frac{\psi + \psi'}{2} = \psi_2 \qquad (3.7)$$

or comply with a measuring method that is less time-consuming. Since the entire curve is not necessary in evaluating Equation 3.6, the small dial sectors may be excluded, and proceed as follows:

1. Focusing on an arbitrary ψ and balancing on the instrument leads.

2. Keep the balance point on the instrument leads and tilt the antenna to $-\psi$. The same angular value cannot be found, but one that varies from ψ. The actual angle is then $\frac{1}{2}(\psi + \psi')$. This process may be repeated for various angles. In this way the symmetry axis is obtained.

3. Since another balancing point may be found on the instrument leads in connection with other ψ, it is now possible to find directly the Δd between two and to calculate φ by Equation 3.6.

Finally, the error calculation that belongs to Equation 3.6 should show what is still to be considered. If the entire differential is again formed, the following equation is obtained as error functions analogous to Equation 3.5.

$$F_1 = \frac{2\left(\sin^2\frac{\psi_1}{2} - \sin^2\frac{\psi_1}{2}\right)}{\left[2\left(\sin^2\frac{\psi_2}{2} - \sin^2\frac{\psi_1}{2}\right) + \frac{\Delta d}{R}\right]^2} \qquad (3.8a)$$

$$F_2 = \frac{\sin\psi_2\,\delta\psi_2 - \sin\psi_1\,\delta\psi_1}{\left[2\left(\sin^2\frac{\psi_2}{2} - \sin^2\frac{\psi_1}{2}\right) + \frac{\Delta d}{R}\right]^2} \qquad (3.8b)$$

$$F_3 = \frac{\left(\frac{\Delta d}{R}\right)^2}{\left[2\left(\sin^2\frac{\psi_2}{2} - \sin^2\frac{\psi_1}{2}\right) + \frac{\Delta d}{R}\right]^2} \qquad (3.8c)$$

and the entire error is expressed as:

$$\delta\varphi = F_1\,\delta(\Delta d) - F_2\,\Delta d + F_3\,\delta R \qquad (3.9)$$

$$\sin^2\frac{\psi}{2} = \sin^2\frac{\psi_2}{2} - \sin^2\frac{\psi_1}{2} \qquad (3.10)$$

The function F_1 and F_3 may again be taken from Diagram 1 if, instead of ψ, an angle is taken from (illegible). The equivalent angle, φ, is to be taken from Diagram 2. Equation 3.10 is a trigonometric equation if it is converted according to $\frac{2\psi_2}{2}$. For that reason the recalculation was easily accomplished. Here again we can say that $\varphi > 6^0$ in order to keep F_1 and F_3 small. A special discussion was required for F_2, because now both angles ψ_1 and ψ_2 can be affected with errors $\delta\psi_1$ and $\delta\psi_2$. Even though it could be assumed that the values are equal, it is still not clear whether the error components are equidirectional or contradirectional, because in connection with the same direction the total error is considerably smaller than in the case of the opposite direction. This decision can be made only when the variation in test results is taken into consideration.

A third evaluation method should now be discussed. If the basic Equation 2.3 is rearranged according to d, we finally obtain the following:

$$\frac{d}{2\sin^2\frac{\psi}{2}} = R\left(\frac{R}{r} - 1\right) = \frac{R}{r}(R - r) = \frac{R}{r}\,o \qquad \frac{d}{2\sin^2\frac{\psi}{2}} = \text{const.} = c. \qquad (3.11)$$

Now it is necessary only to determine c for the various d and the associated ψ values. If d is converted to ψ, it is then possible to carry out a good graphic representation and calculate c from that curve. The point of rotation interval, Z_E, sought for is then expressed as follows:

$$\varphi = \frac{c - R}{c + R} \qquad (3.12)$$

In the graphic representation the specific ψ values must be inserted, first on account of the d values that originate from the various repeated measurements. From that we obtain, to begin with, a cluster of test points. The center of the point cluster is the mean value sought. The curve through the center is then the $d_{(\psi)}$ function, which is to be used in Equation 3.11. It is certain that we obtain

$$c = \bar{c} + \Delta c \qquad (3.12a)$$

Diagram 2

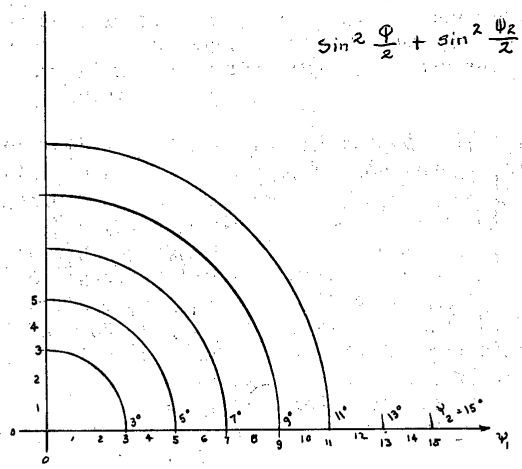

i.e., a constant that is obtained from the mean value of d (ψ) function and the mean deviation in comparison to $\bar{c}$. We will learn about the many applications of this method in the capter on the evaluation of the test results. Except for the error Δc -- the dash should be omitted -- we must still deal with a ΔR error. The complete differential to Equation 3.12 is expressed as follows:

$$\Delta\varphi = \left(\frac{1}{c+R}\right)^2 \Delta R + \left(\frac{R}{c+R}\right)^2 \Delta C$$

$$= \left(\frac{\varphi}{R}\right)^2 \Delta R + \left(\frac{\varphi}{c}\right)^2 \Delta C$$

$$= \frac{c-\varphi}{c+R} + \frac{R-\varphi}{c+R}\,\Delta C \qquad (3.13)$$

The three styles are caused by taking Equation 2.12 into consideration. We can see that the error ΔR has an infinitesimally small part in comparison with Δc, since, of course, $\varphi << R$ ($\frac{\varphi}{R} \approx 1/1$), but it will be $\varphi \approx c$.

Obviously the same method can also be used in the measurement of differences, i.e., with Δd and two accompanying angles, ψ_1 and ψ_2. Then the constant is expressed as:

$$C = \frac{\Delta d}{2\left(\sin^2\frac{\psi_2}{2} - \sin^2\frac{\psi_1}{2}\right)} = \frac{\Delta d}{2\sin^2\frac{\varphi}{2}} \qquad (3.14)$$

Thus it is possible to plot d (ψ) or carry out the above representation and also to work it. Equation 3.13 is, naturally, considered an error function.

In this way we have joined a relatively fast testing method with a good evaluation process. We will also see that properties such as these are important in order to arrive at the correct result logically, i.e., to keep the probable dispersion $\Delta\varphi$ as small as possible.

In conclusion, one more word in regard to the magnitude of Δd or $\delta(\Delta d)$, ΔR or δR and $\Delta\varphi$ or $\delta\varphi$, and $\delta\varphi$. We can assume that by careful measurements the d error amounts to 0.1 to 0.2 millimeters. This will hardly happen in the most adverse cases. The reason should not be anticipated, but a great deal more emphasis should be placed on the results in Chapter 7. The sign of Δd or $\delta(\Delta d)$ remains undetermined. The angle error may be estimated as 0.1 degrees. This value is due entirely to reading error.

The range error is in the order of magnitude of centimeters, because R is, first of all, measured between the point of rotation and, for example, the aperture surface of the transmitting antenna (horn emitter), since of course the position of the radiation center, Z_S, is not known. If we know what it is, then naturally the error is smaller. On the other hand, the influence of ΔR or δR is so small in comparison with the other that an error in measurement of several centimeters really does not matter. Thus, R is measured too small, and for that reason ΔR is always plotted as positive, because $R_{measured} + \Delta R = R$ actually.

4. The Dependence of the Testing Station on Frequency

Matching the sonde (see Chapter 2) to the instrument leads always occurs in one place, i.e., where the phase difference of both bridge branches amounts to exactly π; otherwise the two voltages could not be quenched. That place, however, is uncertain by $K \cdot 2\pi$, because every 2π or after every wavelength a matching is again possible on the instrument leads. In other words, it is not determined by $K \cdot \lambda$ of one of the electrical lengths of the bridge branches (see Figure 1) in comparison to the other. It is not noticed, therefore, when the electrical lengths are not different over the entire wavelength. Therefore the following may be expressed as the matching equation:

$$K 2\pi + \frac{2\pi}{\lambda_o} l_{air} + \frac{2\pi}{\lambda_o} l_{K_1}\varepsilon_r + \frac{2\pi}{\lambda_o} l_M - \frac{2\pi}{\lambda_o} l_{K_2}\varepsilon_r - \frac{2\pi}{\lambda_H} l_H - \Sigma\varphi = \pi \qquad (4.1)$$

in which l_K = The coaxial cable length (Index 1 for the instrument leads and Index 2 for the sonde).

l_H = Length of the hollow waveguide.

l_{air} = Length of the instrument leads (= r).

l_M = Length of the instrument leads from input to the sonde.

ε_r = Relative dielectric constant of the cable dielectrics.

λ_H = Wavelength in the tubular conductor.

λ_{gr} = Minimum lengths of the types of wavelengths used on the tubular conductor.

λ_o = Free-space wavelengths.

$\Sigma\varphi$ = All known phase shifts, e.g., the antenna, crossings, sonde, etc.

Equation 4.1 naturally refers especially to the construction according to Figure 1. In reference 3, this investigation was conducted in a more general way. Here, however, a design instruction on cable length should be published immediately for the testing station, which will then be used in Chapter 8.

Equation 4.1 is multiplied by $\frac{\lambda_o}{2\pi}$ and the following is obtained:

$$K\lambda_o + l_{air} + l_i \varepsilon_r + l_m - l_{K_2} \varepsilon_r - \frac{\lambda_o}{\lambda_H} l_H + \frac{\lambda_o}{2\pi} \Sigma\varphi = \frac{\lambda_o}{2} \qquad (4.2)$$

Now, since $\frac{\lambda_o}{\lambda_H} = \sqrt{1-\left(\frac{\lambda_o}{\lambda_{gr}}\right)^2}$ is valid for the tubular cable, Equation 4.2 becomes:

$$K\lambda_o + l_{air} + l_m + \varepsilon_r (l_K - l_{K_2}) - \sqrt{1-\left(\frac{\lambda_o}{\lambda_{gr}}\right)^2}\, l_H + \Sigma l_u = \frac{\lambda_o}{2} \qquad (4.3)$$

In Equation 4.3, a new length, l_u, has been introduced, i.e., the corresponding unknown phase shifts of the electrical length. For the purpose of simplicity, it is assumed that $l_u = f(\lambda_o)$. If then wavelength λ_o varies by $\Delta\lambda_o$, on the basis of generator oscillations, the result is a shift in of the matching place on the instrument leads. Length $\lambda_o/2$ on the left side of Equation 4.3 does not change because it only characterizes the phase difference between the two voltages on the instrument leads. The following is therefore obtained:

$$K\lambda_o + K\Delta\lambda_o + l_{air} + l_m + \varepsilon_r (l_{K_1} - l_{K_2}) - \sqrt{1-\left(\frac{\lambda_o - \Delta\lambda_o}{\lambda_{gr}}\right)^2}\, l_H + \Sigma l_u = \frac{\lambda_o}{2} + \Delta l \qquad (4.4)$$

First of all, the root expression in Equation 4.4 should be changed somewhat as follows:

$$\sqrt{1-\left(\frac{\lambda_o + \Delta\lambda_o}{\lambda_{gr}}\right)^2} \approx \sqrt{1-\left(\frac{\lambda_o}{\lambda_{gr}}\right)^2 \left(1 + 2\frac{\Delta\lambda_o}{\lambda_o}\right)}$$

$$\approx \sqrt{1-\left(\frac{\lambda_o}{\lambda_{gr}}\right)^2} \left(1 - \frac{\Delta\lambda_o}{\lambda_o} \cdot \frac{\left(\frac{\lambda_o}{\lambda_{gr}}\right)^2}{1-\left(\frac{\lambda_o}{\lambda_{gr}}\right)^2}\right) \qquad (4.4a)$$

If this result is introduced into Equation 4.3, we obtain:

$$K\Delta\lambda_o - l_H \frac{\Delta\lambda_o}{\lambda_o} \frac{(\lambda_o/\lambda_{gr})^2}{\sqrt{1-(\lambda_o/\lambda_{gr})^2}} = \Delta l \qquad (4.5)$$

If K and l_H are dimensioned in such a way that

$$K = \frac{l_H}{\lambda_o} \frac{(\lambda_o/\lambda_{gr})^2}{\sqrt{1-\left(\frac{\lambda_o}{\lambda_{gr}}\right)^2}} \qquad (4.6)$$

a small change in wavelength does not cause a change in the position of the point of matching. That a displacement, Δl, really occurs is based on the assumption $l_u = f(\lambda_o)$. Nevertheless, a reference value is obtained by the above dimensioning equations at least to be able to approximate the minimum of the frequency relationship. According to a small conversion, therefore, the following holds true:

$$K = \frac{l_H}{\lambda_{gr}} \frac{1}{\sqrt{\left(\frac{\lambda_{gr}}{\lambda_o}\right)^2 - 1}} \qquad (4.6a)$$

Details in evaluating Equation 4.6 are treated in Chapter 8.

5. The Influence of Ground Reflections.

In order to be able to observe the most adverse case, it is assumed that the radiation diagrams of both antennas are so broad that the earth is radiated directly just as much. In addition, for the sake of simplicity and also to be able to single out the most adverse case, it is assumed that the same ideal earth is dealt with. Under these assumptions, the following holds true for vertical polarization:

$$E_v = \left| E_{dir} \right| 2 \cos\left(\frac{\pi}{\lambda} s\right) e^{-j\left(\frac{\pi}{\lambda} s + \frac{2\pi}{\lambda} r\right)} \qquad (5.1)$$

and for horizontal polarization:

$$E_h = \left| E_{dir} \right| 2 \sin\left(\frac{\pi}{\lambda} s\right) e^{-j\left(\frac{\pi}{2} + \frac{\pi}{\lambda} s + \frac{2\pi}{\lambda} r\right)} \qquad (5.2)$$

as the receiving field strengths when a indicates the traveling difference between the rays that run directly and through the ground. $|E_{dir}|$ in both cases is the amount of the field strength that takes place directly.

Figure 4

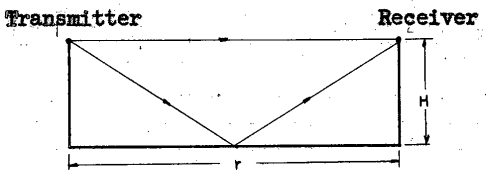

From Figure 4 we can conclude that:

$$s = r\left(\sqrt{1 + \left(\frac{2H}{r}\right)^2} - 1\right) \qquad (5.3)$$

Without mentioning the fact that with a variable r the amplitude of the receiving field strength can vary a great deal, the phase position between the direct and the reflected ray also changes the field strength that enters the receiver, by means of interference. If, therefore, r is changed by $r = d$, with Equation 5.3 we obtain:

$$s + \Delta s = \sqrt{(r+d)^2 + (2H)^2} - r - d \qquad (5.3a)$$

and then $d << r$, we can write

$$s + \Delta s = r\left(\sqrt{1 + \left(\frac{2H}{r}\right)^2 + 2\frac{d}{r}} - 1 - \frac{d}{r}\right) \qquad (5.3b)$$

and

$$\Delta s = d\left(\frac{1}{\sqrt{1 + \left(\frac{2H}{r}\right)^2}} - 1\right) \qquad (5.4)$$

is obtained. Likewise, the same phase angle is in Equation 5.1 and 5.2 with

$$\varphi = \frac{\pi}{\lambda} s \cdot \frac{2\pi}{\lambda} r \qquad (5.4a)$$

and when the antennas are shifted toward each other, it becomes

$$\phi + \Delta\varphi = \frac{\pi}{\lambda}(s + \Delta s) + \frac{2\pi}{\lambda}(r + d) \qquad (5.4b)$$
$$= \frac{\pi}{\lambda} s + \frac{2\pi}{\lambda} r + \frac{2\pi}{\lambda}\left(\frac{\Delta s}{2} + d\right)$$

i.e., $$\Delta\varphi = \frac{2\pi}{\lambda}\left(\frac{\Delta s}{2} + d\right) \qquad (5.5)$$

From Equation 5.5 we can see that angle error $\delta(\Delta\varphi)$ only results from as follows:

$$\delta(\Delta\varphi) = \frac{\pi}{\lambda}\Delta s \qquad (5.5a)$$

or with Equation 5.4

$$\delta(\Delta\varphi) = \frac{\pi}{\lambda} d\left(\frac{1}{\sqrt{1+\left(\frac{2H}{r}\right)^2}} - 1\right) \qquad (5.5b)$$

Since, however, $\frac{1}{\sqrt{1+\left(\frac{2H}{r}\right)^2}} < 1$, we finally obtain

$$\delta(\Delta\varphi) = = \frac{\pi}{\lambda} d\left(1 - \frac{1}{\sqrt{1+\left(\frac{2H}{r}\right)^2}}\right) \qquad (5.6)$$

When d increases, or, expressed differently, when the angle of twist, ψ , increases, angle error increases proportionately to d as long as $d << r$. It is always negative, i.e., a displacement that is measured too small on the instrument leads.

It is H = 1.5 m and r = 8 m, so that

$$d(\Delta\varphi) = -\frac{\pi}{\lambda} d \cdot 0.064 \qquad (5.6a)$$

or the error measurement amounts to $\frac{s}{2} = -d \cdot 0.032$; in connection with d = 10 millimeters it is always -0.32 millimeters. Since this error is too great, arrangements must be made to reduce it. Two possibilities were investigated and considered usable.

The first possibility consists in the use of a reflector being placed in the area where the waves strike the earth. The reflector emits the energy to the side and upward at a steep angle (see Figure 5).

Figure 5

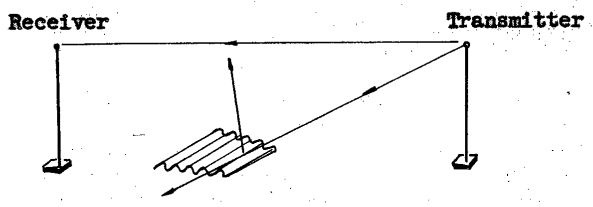

The second possibility consists in reflecting the incoming energy by diffusion, i.e., dispersion. For that reason the earth should not be flat but rather should have elevations which are

$$h > \frac{\lambda}{16\varphi} \qquad (5.7)$$

high. The angle φ is the angle of incidence of the wave to the earth. Equation 5.7 is taken from reference 4 and corresponds to the Rayleigh criterion for diffuse reflections.

In Figure 6 it is shown that a field with such elevations of mud was set up. The mud mounds are about seven to eight centimeters high, have a diameter of about six centimeters, and are about 10 centimeters apart. All the measurements were made with this arrangement.

Figure 6

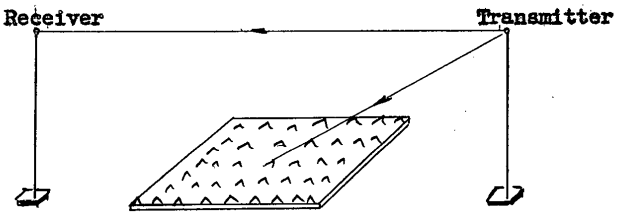

6. The Functional Relationship of Temperature to the Testing Station.

On the basis of various temperature rises of the cable because of the radiation of the sun or the variable temperature of the air, it could be determined that the matching point varied. The correlation with the radiation of the sun was a great deal higher than in the case of the air temperature. The following two conclusions were drawn from that:

a. A fast heat exchange of the radiated cable is to be equalized by means of a heat-insulating cover.

b. Slow temperature changes, e.g., constant heating during the morning hours, cannot be prevented because the temperature balance of the cable cannot be hindered over a long period of time. At least it is not possible with ordinary materials.

At this point, only the results that were attained should be reported. The coaxial cable that was exposed to the radiation of the sun was surrounded by wadding, and the whole thing was wrapped in foil and painted white. Cables that did not have to be right on the ground were buried underground, e.g., the tubular duct and a section of the antenna cable from the receiving antenna to the instrument leads. Diagram 3 shows the results of the last control measurement. Three thermometers were used for it. The first one was packed in the same blue artificial material which was used as the outer protective covering of the coaxial cable and then was placed in the sun. The second thermometer was wrapped in cotton and foil, painted white, and also placed in the direct rays of the sun. The third thermometer was left in the shade without any covering. All three thermometers were suspended 1.5 meters above ground. In that way it was possible to imitate the cable temperature process without having all the precautions (blue cable) and covering (white cable).

The comparison of the three temperature variations with the position of the matching area is then of interest. From Diagram 3 it may be seen that the air temperature and the cable temperature are about the same. Naturally, the higher heat-absorption capacity of the jacket is obvious, because the cable temperature increased from 22.7 to 24.8 degrees, whereas the temperature of the air remained about one degree below that. Furthermore, the variations of the wrapped cable were less affected by the great changes of the sun (blue cable) than by the air. While the cable temperature increased by about two degrees, the matching point on the instrument leads changed by about two millimeters. From Diagram 3 it may be seen that there is a good short-time stability. As already described, the long-duration stability could not be improved any more. For that reason it is important to hold the testing time as short as possible or to select weather when the temperature will not vary a great deal for a long time, i.e., either when the sky is clear or when the cloud cover is uniform. In that respect the second type is even more favorable because in the morning the time when the temperature steadily rises is

used to better advantage because we must find a time for measurements during which the temperature on the average remains rather constant. A thermometer may be placed in the shade to check the air temperature or the variations. If the weather is such that the cloud cover changes rapidly, the measurements are not disturbed by the fast changes in the sunlight. It is possible, nevertheless, for a change to occur in the measuring point because of the continuous increase in cable temperature. Under certain circumstances, a corresponding check must be made before the measurement in order to recheck the long-duration stability.

Diagram 3

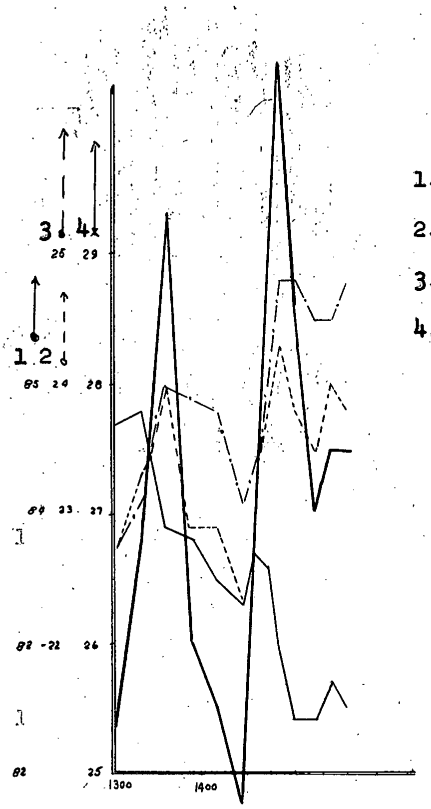

1. Balancing area/millimeters.
2. Air degrees centigrade.
3. White cable.
4. Blue cable.

7. The Influence of Mismatching on the Instrument Leads

Reference 3 described how mismatching, particularly of the received antenna, affects the test results on the instrument leads. It is not shown, however, how great the effect can be and what errors are produced when, for example, m = 0.95. In the following we would like to pursue the calculation along general lines and particularly to discuss the results.

Figure 7

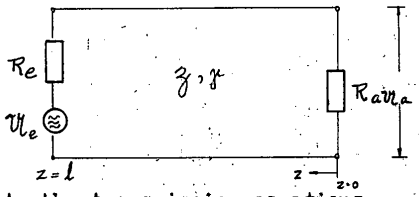

First, we revert to the transmission equations

$$\mathcal{U}_{(z)} = \mathcal{U}_n e^{\gamma z} + \mathcal{U}_r e^{-\gamma z} \qquad (7.1)$$

$$\mathcal{J}_{(z)} = \mathcal{J}_n e^{\gamma z} - \mathcal{J}_r e^{-\gamma z} \qquad (7.2)$$

and maintain that

$$\frac{\mathcal{U}_n}{\mathcal{J}_n} = \frac{\mathcal{U}_r}{\mathcal{J}_r} = \mathcal{Z} \qquad (7.3)$$

is the wave resistance of the line in Figure 7 and

$$\frac{\mathcal{U}_r}{\mathcal{U}_n} = \frac{\mathcal{J}_r}{\mathcal{J}_n} = \mathfrak{w} \qquad (7.4)$$

is the reflection factor when z = 0. In addition, when z = 0, from Equations 7.1 and 7.2 it is

$$\mathcal{R}_a = \frac{\mathcal{U}_o}{\mathcal{J}_o} = \frac{\mathcal{U}_n + \mathcal{U}_r}{\mathcal{J}_n + \mathcal{J}_r} = \mathcal{Z} \frac{1 + \mathfrak{w}}{1 - \mathfrak{w}} \qquad (7.5)$$

or the reflection factor as in Equation 7.4 is expressed as

$$\mathfrak{w} = \frac{\frac{\mathcal{R}_a}{\mathcal{Z}} - 1}{\frac{\mathcal{R}_a}{\mathcal{Z}} + 1} = \frac{\mathcal{R}_a - \mathcal{Z}}{\mathcal{R}_a + \mathcal{Z}} \qquad (7.6)$$

Analogously we define a reflection factor at the beginning of a line, i.e., when z = l, as

$$\mathfrak{w}_e = \frac{\mathcal{R}_e - \mathcal{Z}}{\mathcal{R}_e + \mathcal{Z}} = \frac{\frac{\mathcal{R}_e}{\mathcal{Z}} - 1}{\frac{\mathcal{R}_e}{\mathcal{Z}} + 1} \qquad (7.7)$$

Voltage $\mathcal{U}_e$ may then be calculated as

$$\mathcal{U}_e = \mathcal{U}_{(z+e)} + \mathcal{J}_{(z+e)} \cdot \mathcal{R}_e \qquad (7.7a)$$

If the somewhat tedious calculation is made with the help of Equations 7.1 to 7.7, we obtain two possibilities of solution which should be of additional interest:

$$\mathcal{U}_e = \mathcal{U}_{ne} e^{\gamma e} \left(1 + \frac{\mathcal{R}_e}{\mathcal{Z}}\right) \left[1 - \mathfrak{w}\mathfrak{w}_o e^{-2\gamma e}\right] \qquad (7.8)$$

$$\mathcal{U}_e = \mathcal{U}_{re} e^{-\gamma e} \left(1 - \frac{\mathcal{R}_e}{\mathcal{Z}}\right) \left[1 - \frac{1}{\mathfrak{w}\mathfrak{w}_e} e^{2\gamma e}\right] \qquad (7.9)$$

If this voltage is known, then the incoming ($\mathcal{U}_n$) and returning ($\mathcal{U}_r$) may be calculated as follows from Equations 7.8 and 7.9:

$$\mathfrak{U}_n = \frac{\mathfrak{U}_e \cdot \mathfrak{Z}\, e^{\mp \gamma e}}{(\pm \mathfrak{R}_e + \mathfrak{Z})(1 - [\mathfrak{r}\mathfrak{r}_e]^{\mp} e^{\mp 2\gamma e})} \qquad (7.10)$$

$$r = \qquad (7.11)$$

The voltage at resistor R_a may now simply be determined from Equation 7.10 and 7.11, which, of course, is

$$\mathfrak{U}_a = \mathfrak{U}_{(z=0)} = \mathfrak{U}_n + \mathfrak{R}_r \qquad (7.11a)$$

Finally we obtain the following by subsituting and converting:

$$\mathfrak{U}_a = \frac{\mathfrak{U}_e \mathfrak{Z}}{\mathfrak{R}_e \mathfrak{Z}} \frac{e^{-\gamma e}\,(1 + \mathfrak{r}}{1 - \mathfrak{r}\mathfrak{r}_e e^{-2\gamma e}} \qquad (7.12)$$

Now the voltage distribution along z can also be determined. With Equations 7.1, 7.4, and 7.10 we obtain:

$$\mathfrak{U}_{(z)} = \frac{\mathfrak{U}_e \mathfrak{Z} e^{-\gamma e}}{(\mathfrak{R}_e \cdot \mathfrak{Z})(1 - \mathfrak{r}\mathfrak{r}_e e^{-2\gamma e})} (e^{\gamma z} + \mathfrak{r} e^{-\gamma z}) \qquad (7.13)$$

We can see that $\mathfrak{U}_{(z)}$, in reference to the distribution function along the line, is influenced only by $\mathfrak{r}$. The mismatching at the input (z = 1) of the line finally is taken up by the amplitude (complex amplitude). If the line $0 \geq z \geq 1$ is an instrument lead, then the following is valid:

$$\gamma = j\beta = j \frac{2\pi}{\lambda} \qquad (7.13a)$$

and

$$\mathfrak{Z} = Z \qquad (7.13b)$$

in which λ represents the wavelength of the line, in connection with a coaxial instrument lead $\lambda = \lambda_0 = \frac{c}{f}$, and with a tubular conductor instrument lead it is expressed as

$$\lambda = \frac{\lambda_0}{\sqrt{1 - \left(\frac{\lambda_0}{\lambda_{gr}}\right)^2}} \qquad (7.13c)$$

If we introduce

$$\mathfrak{r} = r e^{j\varphi} \qquad \mathfrak{r}_0 = r_e e^{j\varphi_e} \qquad (7.13d)$$

then

$$1 - \mathfrak{r}\mathfrak{r}_e e^{-j2\beta l} = \sqrt{1 + (rr_1)^2 - 2rr_e \cos\varphi}\; e^{j\psi} \qquad (7.14)$$

with

$$\varphi = 2\beta l + \varphi + \varphi_e \qquad (7.15)$$

$$\psi = \arctan \frac{rr_e \sin\varphi}{1 - rr_e \cos\varphi} \qquad (7.16)$$

Equation 7.13 is then expressed as

$$\mathfrak{U}_{(z)} = \frac{\mathfrak{U}_e Z}{\mathfrak{R}_e + Z} \frac{e^{-j(\beta l - \psi)}}{\sqrt{1 + (rr_e)^2 - 2rr_e \cos\varphi}} (e^{j\beta z} + \mathfrak{r} e^{-j\beta z}) \qquad (7.17)$$

It is analogous to

$$\mathfrak{J}_{(z)} = \frac{\mathfrak{U}_e}{\mathfrak{R}_e + Z} \frac{e^{-j(\beta l - \psi)}}{\sqrt{1 + (rr_e)^2 - 2rr_e \cos\varphi}} (e^{j\beta z} - \mathfrak{r} e^{-j\beta z}) \qquad (7.18)$$

To Equation 7.17 it should be added that the complex amplitude of $\mathfrak{U}_{(z)}$ is not only influenced by the input resistance, which we now very clearly understand, but also by the length of the line because $\varphi = f(e)$. This function disappears, especially when $r_e = 0$.

7.1. The Active Sonde.

Here we should understand that, with the help of a sonde, an additional voltage of an arbitrary amount and phase is connected with the instrument leads. As a prerequisite, it is assumed that the resistance of the sonde, considered in regard to the instrument leads, should be much greater than R_1, R_θ, and Z. In Figure 8 it is again shown how the arrangement is to be understood. The purpose of the calculation, then, is to determine $U_a = f(s)$. According to the superheterodyne principle, the voltage is calculated without

Figure 8

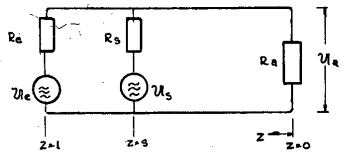

U_s, afterwards U_a without U_e. Both voltages are added at the end and yield $U_a(s)$.

Figure 9

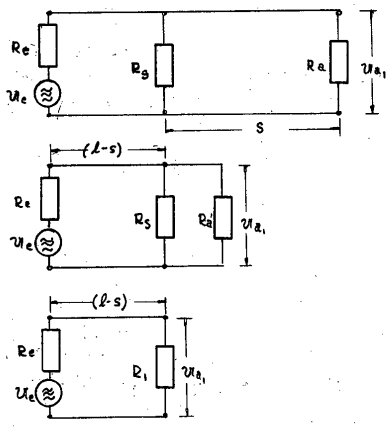

Figure 10

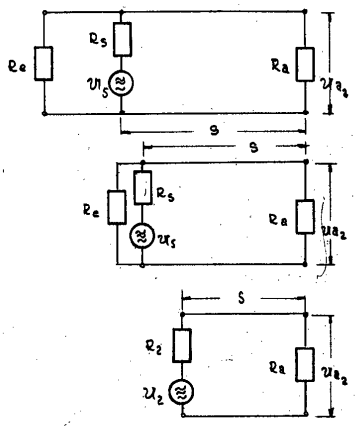

$$U_{a(s)} = U_{a_1} + U_{a_2} \qquad (7.19)$$

The calculation procedure is again illustrated in Figures 9 and 10. We transform R_a according to z = s and with Equations 7.17 and 7.18 we obtain

$$R_{(z)} = Z \frac{\frac{R_a}{Z} + j \tan \beta z}{j \frac{R_a}{Z} \tan \beta z + 1} \qquad (7.20)$$

and, therefore, with z = s,

$$R_a' = Z \frac{\frac{R_a}{Z} + j \tan \beta s}{j \frac{R_a}{Z} \tan \beta s + 1} \qquad (7.21)$$

Resistor R_a should be connected parallel to R_s (Figure 9b). If we assume that $R_a = z$, in order to be able to decouple sufficient energy at the output of the conductor, then our assumption $R_s >> R_a$, i.e., also $R_s >> R_a'$, remains significant. If, on the other hand, the instrument leads at the output are operated nearly at idling or short circuit, there is a danger that at position $\beta_z = \frac{5}{2}$ or odd-numbered multiples of R'_a become very large. We consider our assumption valid, however, and assume that

$$\frac{R_a' - R_s}{R_a' + R_s} \approx R_a' \qquad (7.21a)$$

Then at position z = s we obtain (corresponding to Figure 9c)

$$R_1 \approx R_a' \qquad (7.21b)$$

and, consequently, a reflection factor

$$r_1 \approx r e^{-j2\beta s} \qquad (7.21c)$$

If r_1 is inserted in Equation 7.13, then with $\gamma = j\beta$, as can be expected, we obtain

$$U_{a1} \approx \frac{R_e Z}{R_e + Z} \frac{e^{-j\beta l}(1+r)}{1 - r r_e e^{-j\beta e+2}} \qquad (7.22)$$

This result could also have been read immediately under the conditions stipulated for R j. Here, in particular, it should be shown how the calculation process goes.

In conformity with Figure 10b, we now transform R_e according to z = s, and with Equation 7.20 we obtain the following:

$$R_e' = Z \frac{\frac{R_e}{Z} + j \tan \beta l s}{1 \frac{R_e}{Z} \tan \beta l j + 1} \qquad (7.23)$$

According to the two-pole theory

$$R_2 = \frac{R_e' - R_s}{R_e' + R_s} \qquad (7.23a)$$

and what was said about R_e above again holds true, so that $R_2 \approx R_e'$ can be settled. Voltage U_2 is obtained from

$$U_2 = U_s \frac{R_e'}{R_s + R_e'} \approx U_s \cdot \frac{R_e'}{R_s} \quad \text{for } R_s >> R_e' \qquad (7.24)$$

From Equation 7.12 we now obtain

$$U_{a2} \approx \frac{U_2 Z}{R_e' + Z} \frac{e^{-j\beta s}(1+r)}{1 - r r_e e^{-j2\beta s}} \qquad (7.24a)$$

in which $r_2 \approx r_e e^{-j2\beta(l-s)}$

With Equation 7.14 it is expressed as follows:

$$U_{a2} \approx U_s \frac{Z}{R_s} \frac{\frac{R_e'}{Z}}{\frac{R_e'}{Z} + 1} \frac{e^{-j\beta s}(1+r)}{1 - r r_e e^{-j2\beta l}} \qquad (7.24b)$$

For the expression $\frac{R_e'/Z}{R_e'/Z + 1}$, after several transformations, we receive

$$\frac{\frac{R_e'}{Z}}{\frac{R_e'}{Z} + 1} = \frac{j \frac{R_e}{Z} \sin \beta(l-s) + \cos \beta((l-s)}{(1 + \frac{R_e}{Z}) e^{j\beta(l-s)}} \qquad (7.24c)$$

and finally

$$U_{a2} = U_s \frac{Z}{R_s} \frac{e^{-j\beta l}}{1 + \frac{R_e}{Z}} \frac{1+r}{1 - r r_e e^{j\beta}} \left(\cos \beta(l-j) \frac{R_e}{Z} \sin \beta(l+s)\right) \qquad (7.25)$$

The total voltage is obtained from Equations 7.22 and 7.15 in addition to Equation 7.26

$$U_{a(s)} = \frac{U_e Z}{R_e \cdot Z} \frac{e^{-j\beta l}(1+v)}{1 - v v_2 e^{-j2\beta l}} \left[1 \cdot \frac{U_a}{U_e} \frac{Z}{R_s} \left(\cos\beta(l-s) + j \frac{R_e}{Z} \sin\beta(l-s) \right) \right] \quad (7.26)$$

Whereas the factor in front of the bracket determines only the position of the amplitude and phase, the expression within the brackets shows the function of s, i.e., the position of the sondes.

7.2. Special Use of the Phase Testing Station.

We should like to investigate the term in the parentheses alone in Equation 7.26. In so doing, we proceed from an arbitrary hypothesis, which, however, only insignificantly restricts the validity of the viewpoints following. For that reason the question deals with the distribution of power on the measuring section, and the sonde section is to be considered as phase free and absolutely frequency constant (see Figure 1). In addition, we again maintain the following: U_e and R_e are found at the input of the instrument leads, U_s and R_s are values of the sonde, R_a and $U_{a(s)}$ are given by the receiver connection with the output of the instrument leads.

For the ratio $\frac{U_s}{U_e}$ we write the following:

$$\frac{U_s}{U_e} = u e^{j 2\pi \frac{\Delta l}{\lambda}} = u e^{i \omega \frac{\Delta l}{c}} \quad (7.27)$$

in which Δl is meant to be a difference in length corresponding to Equation 4.4. That means that a frequency change and a phase change are both connected with it, and this is attributed to an error in dimensioning the cabling. If, therefore, the distribution of power is not phase free and, in addition, frequency dependent, then this part should be included with $2\pi \frac{\Delta l}{\lambda}$.

Since R_s should be very large, the sonde must be loosely connected. This resistance may be represented by a capacity as follows:

$$\frac{R_s}{Z} \approx q e^{-j\frac{\pi}{2}} \quad (7.28)$$

The input resistors, R_e, have, first of all, an arbitrary position and size, so that

$$\frac{R_e}{Z} = \mathcal{R} e^{jf} \quad (7.29)$$

introduced. If this is reduced to a lower term in the future, to

$$u q = m \quad (7.30)$$

then the term in the parentheses is expressed as

$$K = 1 + m \cos\beta(l-s) e^{j(\omega \frac{\Delta l}{c} - \frac{\pi}{2})} + mR \sin\beta(l-s) e^{j(\beta - \omega \frac{\Delta l}{c})} \quad (7.31)$$

For various M and M · R, the ellipsoids which result for $K = f_{\beta(l-s)}$ are included in Figure 11. K, however, is not of interest for the information, but rather $|K|$, and in view of that, again, the sharpness of the minimum in order to obtain the most sensitive recording (zero-point equalization).

It can be seen from Figure 11 that M and MR < 1, which corresponds to curve 1, is not taken into consideration. If we follow up the value of K for curve 2, we can confirm the fact that two flat minima appear. Curves 3 and 4, which plainly show the zero points, however, remain. For that purpose, it is

Figure 11

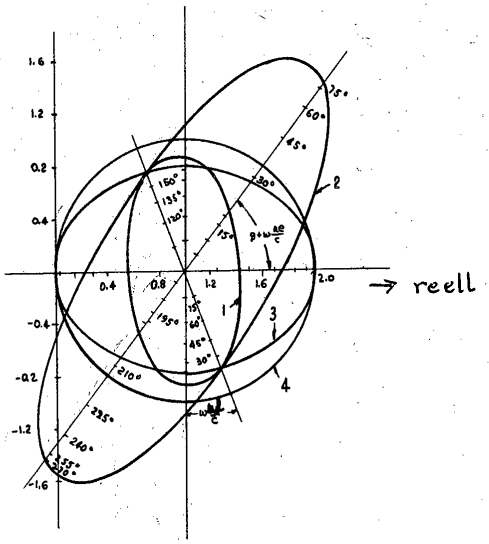

$K = f(\beta(l-s))$

$K = 1 + m \cos \beta(l-s)\, e^{j(\omega \frac{\Delta l}{c} - \frac{\pi}{2})} + mR \sin \beta(l-s)\, e^{j(\varphi + \omega \frac{\Delta l}{c})}$

$0° \leq \beta(l-s) \leq 360°$

Curve	M	MR	φ	$\omega \frac{\Delta l}{c}$
1	0.8	0.6	32°	20°
2	0.8	1.8	32°	20°
3	0.8	1	0°	0°
4	1	1	0°	0°

required to keep $\varphi = \omega \frac{\Delta l}{c} = 0$. We need to think of the instrument leads as lengthened only to the extent that R_e is real. Calculated from that point, however, $\varphi = 0$ and 1, naturally, is greater. In curves 1 and 2, both axes M and M · R are perpendicular, one on top of the other; i.e., the main axes represent the ellipses.

If, then, both antennas are moved toward each other by $\Delta r = -\Delta l$, then $\omega \frac{\Delta l}{c} = 0$, i.e., ellipses are obtained which are symmetrical to the real axis.

If we picture curve 2 as being turned in such a way that it is symmetrical to the real axis, then we can see still more clearly that $|K|$ passes through two minima, and this time they are even symmetrical.

Now we ask the question: How does the position of the zero balance shift on the instrument leads as a function of the change in the interval of the antennas? If it is sufficient to add $\omega\frac{\Delta r}{c}$ to phase angle $\omega\frac{\Delta l}{c}$, then, in connection with a fixed phase position -- e.g., zero equalizing -- between $\mathfrak{U}_s$ and $\mathfrak{U}_e$, a magnitude of Δs could be determined. That is to say, for example, by shifting the sonde, the old phase condition is again restored.

In order to investigate this matter and to answer the question, we look for the extreme values of $|K|$. With Equation 7.31, it is

$$|K| = \sqrt{1 + m^2\cos^2\psi + M^2R^2\sin^2\psi - M^2R\sin^2\psi\sin\varphi + \\ + 2M\cos\psi\sin\omega\frac{\Delta L}{c} + 2MR\cos(\varphi+\omega\frac{\Delta l}{c})\sin\psi} \qquad (7.32)$$

In this,

$$\omega\frac{\Delta l}{c} = \omega\frac{\Delta l}{c} + \omega\frac{\Delta r}{c} \qquad (7.32a)$$

and

$$\psi = \beta(l-s) = \frac{2\pi}{\lambda}(l-s) \qquad (7.32b)$$

The first differential equation is set at zero, and in this way we obtain $\frac{\partial|K|}{\partial\psi} = 0$

$$0 = M\cos\psi\sin\psi(R^2-1) + MR\sin\varphi - 2MR\sin\varphi\cos^2\psi - \\ -\sin\psi\sin\omega\frac{\Delta L}{c} + R\cos\psi\cos(\varphi+\omega\frac{\Delta L}{c}) \qquad (7.33)$$

Equation 7.31 now had to be solved according to ψ. If everything converted to $\cos\psi$, we obtain an equation of the fourth order for $\cos\psi$ which cannot be solved closed. A simplification of the expression, Equation 33, is obtained by $\varphi = 0$. At this point $l - s = 0$, and in the new style it is expressed as $l - s + \Delta s = \Delta s$, i.e., $\psi = \beta\Delta s$. Instead of Δl, we must write $\Delta l'$, and then it amounts to $\Delta L = \Delta r + \Delta l$.

Equation 7.33 therefore obtains the following form:

$$0 = M\cos\psi\sin\psi(R^2-1) - \sin\psi\sin\omega\frac{\Delta L}{c} + R\cos\psi\cos\omega\frac{\Delta l}{c} \qquad (7.34)$$

This equation has as yet not been solved closed for ψ. For $R \to 1$, i.e., $\frac{|R_e|}{Z} \to 1$, or the new source of supply, $\frac{R_e}{Z} \to 1$, the first term goes toward zero and, consequently, only slightly into the final result. We tried an approximate solution with

$$\sin\psi\sin\omega\frac{\Delta L}{c} = R\cos\omega\frac{\Delta L}{c}\cos\psi \qquad (7.35)$$

$$\tan\psi = R\cot\omega\frac{\Delta L}{c}$$

For R = 1, i.e., 100 percent matching, we obtain

$$\psi = \omega\frac{\Delta l}{c} + \omega\frac{\Delta r}{c} - K\frac{\pi}{2} \qquad (7.35a)$$

with K = 1, 3, 5, 7, etc., or

$$\Delta s = \Delta l' + \Delta r - K\frac{\lambda}{4} \qquad (7.35b)$$

The result shows that with R = 1 there is complete synchronization between Δr and Δs. As soon as $R \neq 1$, this is no longer the case. Nevertheless, our calculation shows that the result is independent of M. That means for K (see

Figure 11) the circle is about the value 1. There we introduce curve 2 by R = 1, i.e., M = MR = 0.8, and then one could also omit φ and obtain a circle. With M = 1, of course, we obtain a zero balance, but not with M < 1. Then we wanted to allow a small mismatching and to calculate the maximum error which is opposite to R $\doteq$ 1 with regard to Δs. If we say $X = \omega \frac{\Delta L}{c}$, then Equation 7.35 is written (see also Figure 12) as:

$$\tan \psi = R \tan \left(\frac{\pi}{2} - x\right) \qquad (7.36)$$

and the error that is sought is

$$\eta = \psi - \left(\frac{\pi}{2} - x\right) \qquad (7.36a)$$

i.e.,

$$\eta = \text{arc tan} \left[R \tan \left(\frac{\pi}{2} - x\right)\right] - \left(\frac{\pi}{2} - x\right) \qquad (7.36b)$$

Figure 12

The maximum deviation, i.e., η_{max}, is obtained from $\frac{\delta \eta}{\delta x} = 0$ to $\eta_{max} = 2 \arctan \sqrt{R}$.

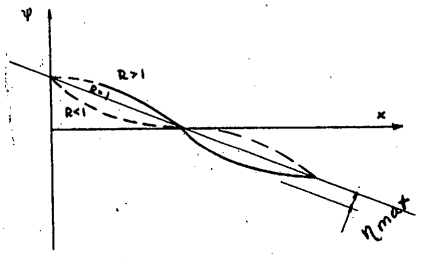

Diagram 4

Maximum Error as a Function of Mismatching

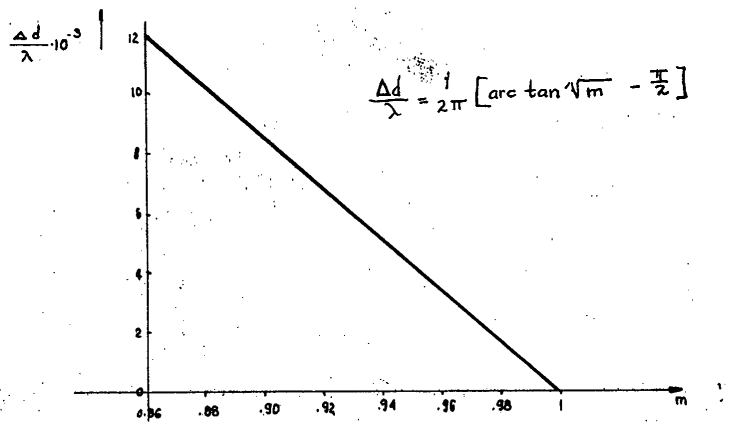

Since $R = \frac{R_e}{Z}$, we can actually also use m as the matching. Naturally, we must take into consideration that the instrument leads are lengthened to the point that R_e is real and a minimum. That does not influence the considerations in the least, and for that reason we may write

$$|\eta_{max}| = |2 \arctan \sqrt{m} - \frac{\pi}{2}| \qquad (7.37)$$

It should again be stressed that Equation 7.37 is valid only for $m \rightarrow 1$. It is, therefore, $|\eta|_{max}$, the amount of the maximum angle of error that occurs between the actual and the erroneous sonde position in matching to the instrument leads. Consequently, it is expressed as

$$\eta_{max} = \frac{2\pi}{\lambda} \Delta d_{max} \qquad (7.37a)$$

In Diagram 4, $\frac{\Delta d_{max}}{\lambda}$ is represented as a function of λ. If we accept that, matching amounts to m = 0.95. Normally that is a quality that requires no further explanation. It may be read as $\frac{\Delta d_{max}}{\lambda} = 4.15 \cdot 10^{-3}$. The wavelengths are λ = 10 centimeters, i.e., $\Delta d_{max} \approx 0.415$ millimeters. This is an error that should, under no circumstances, be allowed.

It must therefore be very carefully matched, and one should take the trouble of setting m > 0.98. Of course, another restriction occurs here. The frequency of the generator may change only very little; otherwise, the adjusted match possibly no longer exists during the specific phase measurement.

8. The Arrangement of the Test Station.

The entire installation is out in the open. It is arranged according to the principle shown in Figure 1. In Figure 13 it may be seen that the two antennas (horn emitter) stand on a paved foundation 10 meters long and two meters wide.

Figure 13

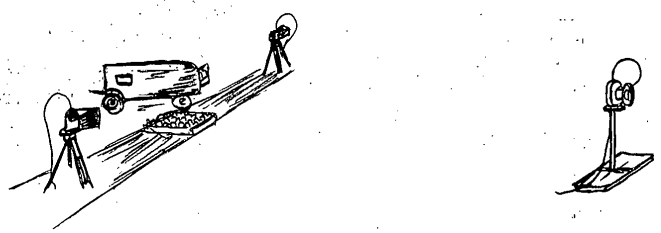

The auxiliary antenna is fixed on a tripod; the antenna that is to be tested is on a stand, which allows it to be rotated and translated. It stands about 1.5 meters above the ground. In order to hinder the ground reflection, the mounds of sand and mud mentioned in Chapter 5 are taken into consideration. All the measuring instruments, generators, amplifier, etc. are in a vehicle, which is set up at the top of the measuring section. With the exception of the power-supply cable, all the coaxial cables that are not underground are thermally insulated in order to equalize fast thermal variations.

The circuit arrangement of the testing station is shown completely in Figure 14. From that it may be seen that a section of the sonde cable consists

Figure 14

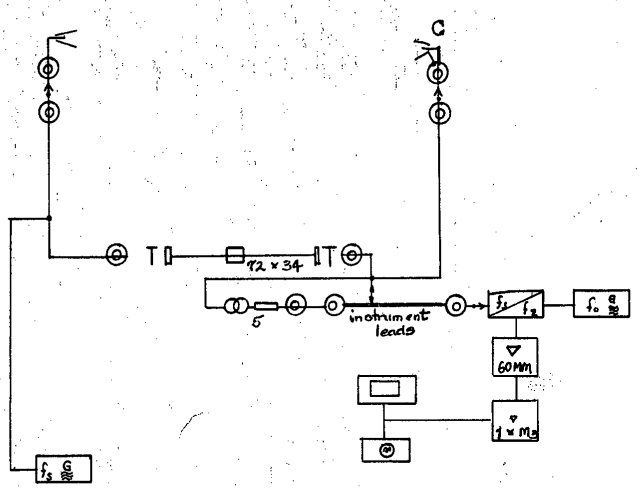

of a tubular conductor. This measure had to be taken, because otherwise the sonde voltage is too low. Even if a certain equalization is possible by inserting an attenuator pad in the antenna cable, the attenuation still cannot be raised high enough to induce the uniformity of the two compensating voltages, because then the balancing sharpness suffers a great deal. A laminated core transformer was inserted in order to adjust a satisfactory matching to the instrument leads.

The signal is a result of the increase in sensitivity by means of mix reception. Harmonic wave mixing is generally the result. The accompanying intermediate-frequency amplifier (60 megacycles) gives its demodulated signal to a small-band (band width $\approx$ 50 cps) one-kilocycle amplifier, so that only the 1000-cps ground wave is filtered out of the square-wave modulated carrier oscillation with a frequency of f_s. In this way the signal is removed from the noise, that is, additional sensitivity is reached. The modulation frequency of one kilocycle is very favorable, in that all 50-cycle hum effects or hum loops can be suppressed to a minimum by skillfully mounted suppressors. The true signal is then given on an oscillograph, which is best suited for monitoring, and a microvoltmeter (red and black) in order to obtain a plain signal of the minima.

The testing station is set up for a frequency range of 4.3 to 2.5 gigacycles, i.e., a wavelength range of seven to 12 centimeters. The frequencies are given by the tubular conductor. Amplification is always possible in both directions as soon as suitable cables are available. The coaxial cables have a characteristic impedance of 70 ohms (large cross section, 5/16), and they are serviceable down to a wavelength of approximately 4.5 centimeters without restriction. Of course, a test must be made to determine whether the cable attenuation is not too high and, if necessary, put more tubular conductors into service.

8.1 The Wiring of the Testing Station (λ = 7 to 12 Centimeters).

As mentioned, the testing station was originally installed for this range because enough tubular conductors with a cross section of 72 by 34 millimeters were available.

Table 8.1

$\frac{\lambda_o}{cm}$	$\frac{\lambda_H}{\lambda_o}$	$\frac{l_H}{m} / \frac{\lambda_H}{\lambda_o}$	$K\lambda_o + \frac{l_H}{\lambda_H/\lambda_o}$
12	1.81	6.5	21.28 m
11	1.555	4.54	18.22 m
10	1.390	8.46	16.36 m
9	1.280	9.19	15.05 m
8	1.207	9.75	13.93 m
7	1.143	10.3	13.48 m

Table 8.2

$\frac{\lambda_o}{cm}$	$\frac{1}{\sqrt{(\lambda_{gr}/\lambda_o)^2 - 1}}$	K	$K\frac{\lambda_o}{m}$
12	1.509	123	14.78
11	1.189	97	10.68
10	0.966	79	7.9
9	0.800	65.3	5.86
8	0.666	52.4	4.18
7	0.557	45.5	3.18

$$K = \frac{l_H}{\lambda_{gr}} \cdot \frac{1}{\sqrt{(\lambda_{gr}/\lambda_o)^2 - 1}} \qquad \frac{\lambda_H}{\lambda_{gr}} = \frac{11.7\ m}{0.144\ m} = 81.6$$

Because of the dielectrics involved, the coaxial cables are about 1/0.66 longer electrically than geometrically. The tubular conductor, on the other hand, is shorter by the factor λ_o/λ_H. Table 1 shows the function of the electrical length on the wavelength λ_o. The factor K, which must have a specific magnitude as a consequence of the theoretical investigations, in order to realize a minimum frequency dependence of the testing station, is presented in Table 2. Since the tubular conductor appears to be so short, it is significant to propose K . λ_o to this aspect. The final lengths may again be found in Table 1. The lengths given in Figure 15 are all measured according to Equation 4.3, in which, of course, l_u = 0 or $\frac{\lambda_o}{2}$. The values indicated in Figure 15 hold true for a testing distance of eight meters. In order to use as few auxiliary cables as possible, no determining value was placed on absolute uniformity. The remaining differences of fewer wavelengths are to be settled insofar as is really necessary. Experience has shown that the quoted values (Figure 14) are completely sufficient. If, nevertheless, too great an instability of the matching point should be observed as a function of the frequency, then an attempt must be made to place the emitters closer together or farther apart.

All the cables at the testing station consisted of the following:

l_1 = 1.85 meters. l_3 = 1.85 + 0.95 + 1.95 meters.

l_2 = 0.95 meters. l_4 = 12.7 meters.

for λ_o = 12 centimeters. In changing to λ_o = 11 centimeters, only l_1 and l_2 were exchanged. In connection with λ_o = 10 centimeters, both $l_1 + l_2$ = 2.8 meters are connected and power is immediately supplied to the antenna. The intermediate sections having a length of 1.2 and 0.37 meters are available as extras.

All the cables are painted white in order to make them distinguishable from the others on either side. The 12.7-meter-long cable is buried in the ground in places. The cables that are in the air are completely insulated thermally. Absolute care must be taken that the insulations are always in perfect condition.

The tubular conductor is completely underground.

Figure 15

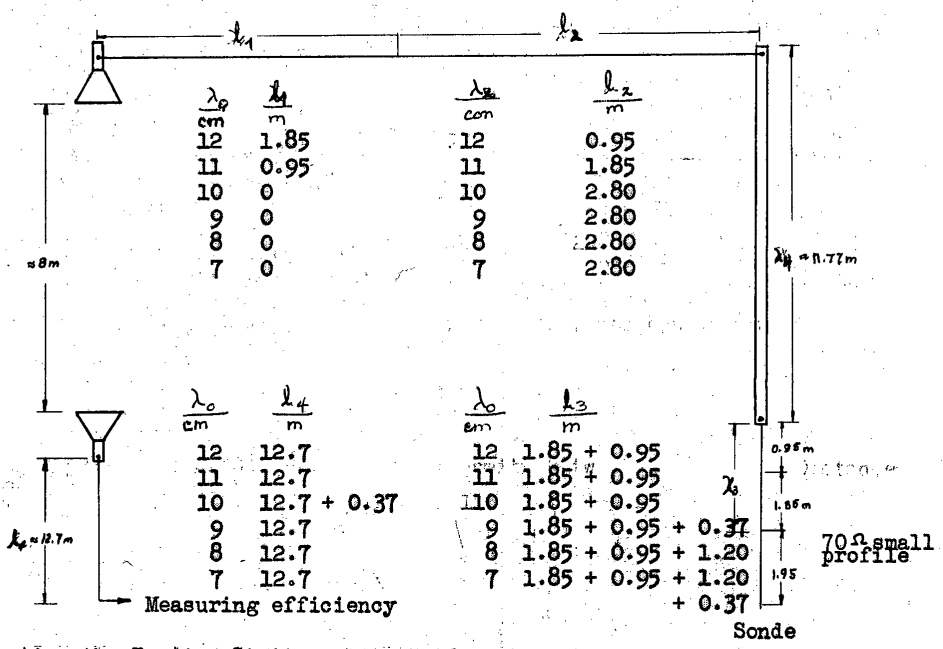

8.2 Testing the Testing Station as to Uniformity Between the Antenna Distance and the Matching Position Changes.

If one of the two antennas is moved, the matching point must move by the same amount on the instrument leads (coaxial). The topic was treated in detail in Chapter 7, where it was shown that this was not the case when the instrument was mismatched on the input side. Two examples should show how matchings of m = 0.95 and m ≈ 0.99 work out. An absolute matching of the error maxima between the calculation and the experiment should not be expected, because, of course, the solution of Equation 7.35 is valid only if it is assumed that m $\longrightarrow$ 1.

The functions $\Delta d = f(a)$ are plotted in Diagram 5. The evaluation must be carried out in such a way that Δd_{max} is determined from the symmetrical line. In this way we obtain the following:

$$m = 0.95 \quad \frac{\Delta d_{max}}{\lambda_0} = \frac{1}{120} \cdot 8.35 \cdot 10^{-3} \qquad m = 0.99 \quad \frac{\Delta d_{max}}{\lambda_0} = \frac{0.3}{120} = 2.5 \cdot 10^{-3} \quad (8)$$

From the approximate solution (Diagram 4), the following is obtained:

$$m = 0.95 \quad \frac{\Delta d_{max}}{\lambda} = 4.1 \cdot 10^{-3} \qquad m = 0.99 \quad \frac{\Delta d_{max}}{\lambda} = 0.8 \cdot 10^{-3} \quad (8.1)$$

i.e., considerably smaller values. From this it may again be deduced that a satisfactory matching must be produced. The good matching that was once obtained is, naturally, valid for one frequency and for that reason it is of the utmost importance to use a generator that has a high frequency stability.

Diagram 5

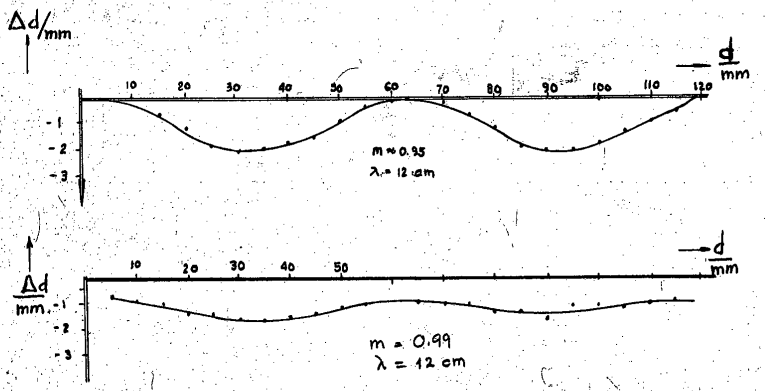

8.3. Instruments Used (see Figure 14).

1. A klystron calibrating-transmitter test oscillator, manufactured by Siemens, was used as the transmitter generator (f_s). Wavelength changes in connection with λ = 120 millimeters can be determined in the course of several hours between λ = 119.7 and 121 millimeters. The stability ($\approx 10^{-2}$) is obviously sufficient because serious difficulties cannot be determined. It seems significant to allow the generator to run for about a half hour to an hour. If the occasion should arise, improvements can be obtained with a magnetic stabilizer.

2. The coaxial instrument leads were designed by Rafena. In addition, an aperiodic sonde connection was used (made at the plant). Low variations in intensity that appear during the measurements -- e.g., on the basis of the radiation diagram -- can be corrected without any difficulty by changing the sonde depth. The position of the matching point is not at all or not noticeably influenced by this.

In order to test the matching, the standard keying head was used, the mixer (receiver) was off, and the transmitter was turned on with the f_s frequency. After being set on m = 1 with the help of the disk compensator -- other transformers are also applicable -- the transmitter may no longer be changed, or the matching cannot be correct by a frequency variation.

3. A triode generator was used for a superheterodyne generator of the f_o frequency (λ = 9 to 16 centimeters or 18 to 33 centimeters). In order to increase the frequency stability, it was operated over a magnetic voltage stabilizer.

4. The receiver and the 60-megacycle amplifier and the one-kilocycle amplifier are all construction elements that represent test designs or models that were developed.

There is nothing particularly noteworthy about the other instruments. It appears suitable to operate the one-kilocycle amplifier also over a voltage stabilizer.

9. Evaluation of Test Results.

Measurements at λ = 12 and 8 centimeters were carried out on a horn emitter. While $x_{(\psi)}$ was plotted in connection with the larger wavelength (see Chapter 3), with only eight centimeters the faster testing method with $\Delta d_{(\psi_1,\psi_2)}$ could be used. The third evaluation method, with regard to constant c (see Equation 3.12), was used as a comparison in both cases. In order to avoid continuous description of the individual methods, they are simply numbered, naturally in the sequence in which they were mentioned. Evaluation according to Equation 2.3 and the accompanying test method, i.e., the plotting of $x_{(\psi)}$, is designated I. The second method, in which Equation 3.6 is used, is therefore designated II. The evaluation of constant c may be accomplished in both cases, as we know; therefore C I and C II designate the evaluation method.

For λ = 12 centimeters, therefore, begin with method I and take Diagram 6 into consideration. There are four curves to measure, which were measured without any change in the test set-up. It therefore required several hours before all the values from the four curves could be measured. From the deviation in the test values, it is obvious that long-duration effects are present. The sequence of the numerals corresponds to the survey sequence, so that one must suppose that the temperature changes during the morning and afternoon are

mutually subject to the position of the curves. Beyond that, the curves are also not congruent, obviously, because of the relatively long measuring time even for only one curve. In addition, short-duration effects are to be picked out because the measuring points are not all on the curve.

The evaluation is made as described in Chapter 3, with the aid of Figure 3. Table 9.1 contains the old φ values which were calculated according to I and II from the curves in Diagram 6. In this connection it should also be noted that values ψ_1 and ψ_2 represent round values, which actually do not yield any whole numbers when the angle is determined according to Equation 3.7. In the calculation, of course, this must be taken into consideration, because the angle error, especially, plays a large part in the final result. Nevertheless, for comparison a review such as that in Table 9.1 is sufficient.

Table 9.1

Angle ψ_1°	Angle ψ_2°	Curve 1	Curve 2	Curve 3	Curve 4	Equivalent angle φ°	$\bar{\varphi}$/mm value
0	7	1045	1045	1008	1032	7	1038.75
0	9	1039	1060	1029	1050	9	1044.5
0	11	1040	1058	1058	1050	11	1051.5
0	13	1061	1093	1042	1056	13	1063.0
0	15	1058	1053	1049	1058	15	1054.5
7	9	1071	1088	1065	1076	5.64	1075.0
7	11	1060	1069	1059	1064	8.5	1063.0
7	13	1069	1070	1056	1064	10.96	1064.75
7	15	1052	1058	1060	1061	13.21	1057.75
9	11	1052	1052	1051	1055	6.32	1052.5
9	13	1065	1040	1056	1061	9.38	1055.5
9	15	1050	1050	1061	1060	11.95	1055.25
11	13	1080	1080	1055	1068	6.9	1070.75
11	15	1059	1050	1062	1060	10.13	1057.75
13	15	1020	1028	1068	1057	7.36	1043.25

The table begins with angles from 7°, because an evaluation among them, on the basis of the error calculation, is senseless from the beginning. The smallest φ value is 1008 millimeters, the largest 1093 millimeters; therefore there is a spread range of 85 millimeters over all 60 results. It is noteworthy that both values are in the first group ($\psi_1 = 0$). The dispersion in the other groups, taken all together, is only 68 millimeters. For this reason alone, a higher accuracy is attributed to method II, although an evaluation such as that is permitted only to a limited extent by the testing method used here. Measurements for λ = eight centimeters were made exclusively according to method II. We will discuss this further, later on.

The last column of the table contains the arithmetical mean value of φ that belongs to each line. From an analysis of the errors (see Diagram 1), it is possible to make a selection from the 15 mean values in a significant manner and to consider the mean value as the final result. Accordingly, all the values that were measured with $\varphi > 10$ degrees are taken into consideration. These are seven values from Table 9.1, which again deliver a mean value of

$$\varphi = 1057.8 \text{ millimeters} + 6.25 \text{ millimeters} - 6.30 \text{ millimeters} \qquad (8.2)$$

ion.

ion.

with the indicated scatter deviations. Table 9.2 was compiled in order to obtain a general view of the value for $\Delta\varphi$ that originated from the error calculation from which, first of all, F_1, F_2, and F_3 result, and, finally, the individual error influences.

Table 9.2

Error Factors								Error Values				
$\psi_1°$	$\psi_2°$	φ'	$\frac{d}{R}\frac{\Delta d}{R}$	F_1 ϱ^3	F_2+ ϱ^{-3}	F_2- 10^{-3}	F_3 mm	$dR=\Delta d$ mm	ψ $+mm$	ψ $-mm$	R mm	$\Delta\varphi$ $+mm-$
0	7	7	1.0	0.102	1.65	-	0.014	10.2	25	-	0.42	36 -
0	9	9	1.7	0.060	0.80	-	0.014	6.0	20.4	-	0.42	27 -
0	11	11	2.5	0.040	0.40	-	0.014	4.0	15.2	-	0.42	20 -
0	13	13	3.5	0.026	0.20	-	0.015	2.6	10.6	-	0.45	14 -
0	15	15	4.7	0.018	0.18	-	0.015	1.8	12.8	-	0.45	13 -
7	9	5.64	1.0	0.142	8.46	1.050	0.030	14.2	128.5	15.90	0.90	143 30
7	11	8.50	1.5	0.068	1.71	0.374	0.015	6.8	39.0	8.54	0.45	47 16
7	13	10.96	2.5	0.040	0.73	0.140	0.014	4.0	27.8	5.34	0.42	32 10
7	15	13.21	4.0	0.025	0.50	0.180	0.018	2.5	30.3	10.90	0.54	34 15
9	11	6.32	1.0	0.122	6.210	0.621	0.020	12.2	24.9	9.43	0.60	107 22
9	13	9.38	2.0	0.055	1.405	0.246	0.017	5.5	42.6	7.50	0.51	49 14
9	15	11.95	3.0	0.035	0.700	0.170	0.014	3.5	31.9	7.74	0.42	36 12
11	13	6.90	1.0	0.104	6.050	0.490	0.015	10.4	91.6	7.44	0.45	102 18
11	15	10.13	2.0	0.049	1.535	0.267	0.013	4.9	46.6	8.10	0.39	52 13
13	15	7.36	1.2	0.090	3.045	0.405	0.018	9.0	55.5	7.36	0.54	65 17

Error: Δd b on $\delta(\Delta d) = 0.1$ mm $\quad \Delta\psi = 0.1°$ $\quad \Delta R = 30$ mm

Diagram 6

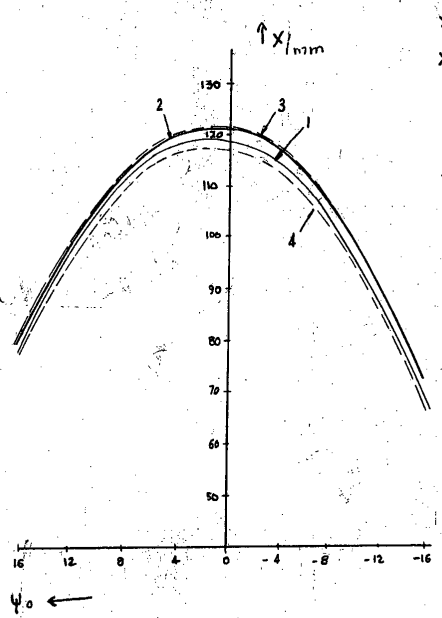

x = f(φ)

X = Balance spot on the instrument lead.

λ = 12 centimeters.

R = 8716 millimeters.

The ratios $\frac{d}{R}$ or $\frac{\Delta d}{R}$ are round numerical values which result from Diagram 6. Plus and minus signs mean that $\delta\varphi_1$ and $\delta\varphi_2$ are sometimes equal and sometimes unequal. Accordingly, the error portions also drop out.

Diagram 7

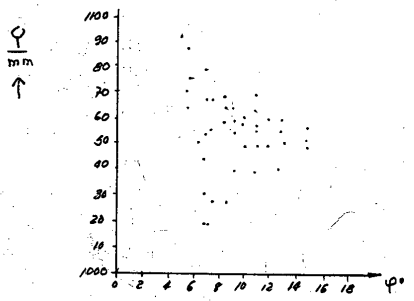

Diagram 8

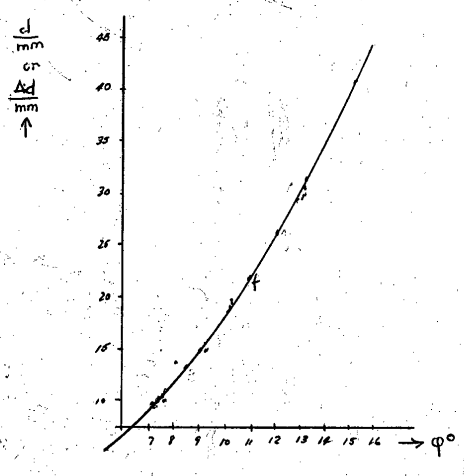

From the values for $\Delta\varphi$ we can see that method II actually hardly causes a significant reduction in the errors. In addition, it is again as large (assuming it is the ψ_1 value) as the current value which can be determined from $\bar{\varphi}$. It is very important to recognize, however, that the same counted seven values produce the smallest values for $\Delta\varphi$. From this we can conclude that measurements below ψ = 10 degrees are hardly of any practical interest, and one knows more exactly whether $\frac{d}{R}$ or $\frac{\Delta d}{R}$ is smaller, because the F_2 value is not really very high in connection with $\varphi > 7°$.

Another method of understanding which value φ is the most probable to take consists in plotting suitably calculated φ values over the equivalent angle φ. This took place in Diagram 7. It is very easy to see there that with small angles the distribution of the value is extraordinarily high and that it decreases after larger angles. The following may be concluded from that representation:

$$\varphi \approx 1054 \pm 4 \text{ millimeters.} \qquad (8.3)$$

This representation shows especially well the outside 1093 millimeters at 13 degrees, which, of course, can play an essential part in the result by a simple method.

We would now like to proceed to method III. Diagram 8 was completed for that purposes. Therefore, d or Δd (on the basis of II) is plotted over φ. If a curve is drawn through the cluster of dots, then c can be determined. Table 9.3 shows the result. A relatively good agreement of the c value is obtained. Its average value is c = 1195.6 millimeters + 6.4 millimeters - 5.6 millimeters.

Table 9.3

ψ	$\sin^2\frac{\varphi}{2}$ 10^{-3}	d or Δd mm	c m
6	2.745	6.60	1.202
8	4.875	11.60	1.190
10	7.625	18.20	1.193
12	10.910	26.00	1.190
14	14.810	35.40	1.193

According to Equation 3.12 with R = 8716 millimeters, we obtain φ = 1050.5 + 5 millimeters - 4.3 millimeters. It was noticed that the results for φ displayed a decreasing tendency. It is, however, just as noteworthy that (see Table 9.3) the $\psi_1 = 0°$ group in actual numbers is about 103 millimeters and comes under that, while the other groups, up to the last, produce greater values. That means also, that it is not easy to decide which of the φ values calculated is probably correct. It is obvious for

$$\varphi = 1054 \pm 4 \text{ millimeters} \qquad (8.4)$$

to be given as final, because it is exactly in the middle, but even at that it is not 100 percent certain.

The interval of the center of the radiation from the aperture is now very easily calculated. The interval of the aperture point of rotation is 1086 millimeters, i.e., the center is about 32 millimeters $\pm$ 4 millimeters behind the aperture. We would like to call distance a:

$$a = 32 \pm 4 \text{ millimeters, for } \lambda = 12 \text{ centimeters.} \qquad (8.5)$$

Now we turn to the test results for λ = eight centimeters. As already pointed out, only method II was used, and it required about 15 to 20 minutes to conduct the tests. Table 9.4 shows the results.

Table 9.4

ψ°	x/mm	ψ_r°
- 5 + 4.9	129.08	4.95
- 10 + 9.9	115.20	9.95
- 15 + 14.9	93.00	14.95
- 20 + 19.95	62.16	19.95

Table 9.5

ψ_1°	ψ_2°	φ	d/mm	$\frac{\Delta d}{R} 10^{-3}$	φ/mm
4.95	9.95	8.65	13.88	1.545	1071
4.95	14.95	14.10	36.68	4.020	1055
4.95	19.95	19.30	66.92	7.450	1050
9.95	14.95	11.18	22.20	2.472	1045
9.95	19.95	17.20	530.40	5.905	1045
14.95	19.95	13.25	30.84	3.438	1046

R = 8991 millimeters
λ = 8 centimeters

From these four test values, six results may be calculated, which are then to be subjected to more detailed investigation. The values that belong together are compiled in Table 9.5. The same tendency for φ is again noted which was already characterized for method II in connection with λ = 12 centimeters. The values from the top move toward the probably correct value of approximately 1046 millimeters. Here large equivalent angles were always used in order to keep the error small from the beginning. In addition, this method requires little testing time, so that long duration effects may be considered connected. Nevertheless, we would again like to look at the error table, Table 9.6, in which it is shown that only the latter of both the first groups and the latter result are considered in the final result. The following is obtained as a mean value of these three values.

Table 9.6
Error Share

φ°	Δd mm	$+\psi$ mm	$-\psi$ mm	R mm	$\Delta\varphi$ + mm	$\Delta\varphi$ - mm
8.65	6.800	37.50	12.50	0.4300	46.5	20.0
14.10	2.580	18.55	9.29	0.4150	22.0	12.6
19.30	1.388	12.32	7.35	0.4105	14.4	9.4
11.18	4.150	36.90	7.29	0.4040	41.4	12.0
17.20	1.740	18.45	6.05	0.4060	20.7	8.0
13.25	3.000	37.00	5.16	0.4090	40.4	8.5

For evaluation by method II, there is, as noted above, only a single series of significant measurements. No diagram similar to Diagram 8 can be evaluated here. Otherwise, $\frac{\Delta d}{2 \sin^2 \varphi_2} = c$ can be calculated from the measurement values in Table 9.5 and the values in Table 9.7 can be reached. If all the c values are calculated together in the same way, since the φ numbers are the same for small as for large angles, the arithemtic mean value obtained is

Table 9.7

φ°	$\sin^2 \frac{\varphi}{2} \cdot 10^{-3}$	c/m
8.65	5.70	1.192
11.18	9.54	1.165
13.25	13.22	1.166
14.10	15.05	1.200
17.2	22.35	1.196
19.3	28.05	1.192

c = 1.185 meters + 15 millimeters
$\mp$ 19 millimeters
and from this we obtain the following with Equations 3.12 and 3.13:

φ = 1049 $\pm$ 13 millimeters

From this result, it is possible to see that a simple test series is in no way adequate for method III in order to be able to reach a reasonable conclusion.

Nevertheless, we can determine in the end that the radiation center is moved toward the inside of the horn emitter when the wavelength decreases or when the frequency increases. This is a tendency that was expected. The fluctuation between $\lambda = 12$ centimeters and $\lambda = 8$ centimeters amounted to six to eight millimeters. The center of radiation, therefore, was about 25 millimeters behind the aperture. In addition, it is maintained that it is advisable to conduct these measurements with a great deal of patience because this process is extremely susceptible to errors (see also the results in reference 1), and the author was not able to find a better method.

10. Operating Instructions.

From the subject treated in the previous chapter, a type of measuring program may be compiled in order to permit as satisfactory as possible an operation.

1. A paved area on which to set up the antenna is necessary. The auxiliary antenna is mounted on a tripod. The antenna to be tested is mounted on a mast. (?)

2. The truck with the testing instruments should not be parallel to the test range, but at the top provided for it, in order, to the greatest extent possible, to prevent damaging reflections from the truck. The measuring station should be so arranged that a side road can be used for parking the truck.

3. The cables must all be provided with thermal insulation and measured in accordance with the data presented in Chapter 8, Figure 15. When necessary, corrections should also be made only in accordance with the specifications given in Chapter 8 or perhaps in Chapter 4. (In this connection, see also Chapter 6.)

4. Adjust the desired frequency. The frequency is produced by a generator with a high-frequency constant. With this frequency, the matching on the antenna side can be controlled by the instrument leads. By means of a disk compensator, it is possible to adjust the matching to $m > 0.98$ (maximum of $m = 1$). Thereafter the generator is again to be connected with the power cable.

5. Mount the aperiodic connection on the instrument leads. The precision instrument leads by Rafena were used. The sonde is to be disregarded in the calculation (loose connection!) and the oscillator frequency, f_o, is to be regulated so that the maximum voltage is indicated on the indicating instrument or on the oscillograph. If necessary, the modulation frequency is also to be adjusted on the test generator in order that exactly 1000 cps are produced. The sondes are now slowly screwed in, and thus the test slits are slowly moved. The sonde and the test slits must be adjusted in such a way that it is possible to compensate the 1000 cps voltage completely.

6. The frequency of the test generator, i.e., f_s, changes slightly but definitely. This happens the best in klystron generators through changing the reflector voltage. The compensations then will have to be corrected only at $f_s \pm \Delta f_s$. If a change in location is connected with the correction, then a recheck must be made to determine whether other matching

points have a slight location-frequency function, which is n λ_o above or below. Under certain circumstances, smaller changes in interval R or r must be made. It could also happen that the sonde adjustment must be changed with each frequency change in order to obtain a zero balance. Moreover, a check is to be made to determine whether a sonde depth change causes a change in position. Generally this is not the case, but nevertheless a check is always recommended. The sonde should not go too far into the instrument lead; otherwise disturbances and false test results can be expected.

7. Again adjust the desired frequency, f_s, in order that the match originally produced is again present. It is recommended that the matching be controlled. It is more important to have perfect matching than an absolutely independent frequency matching point. The latter, in principle, is hardly attainable.

8. Recheck the linearity between test antenna displacement and matching reference shifting. Nevertheless, an attempt is to be made to install the antennas one on top of the other as carefully as possible (note 9, below). In order to make the recheck, it is necessary to move the test antenna at least a half wavelength at an interval of approximately $\frac{\lambda}{10}$ and to pursue the matching point. The evaluation of this control test is conducted according to the model in Chapter 8, Diagram 5.

9. The test antenna is adjusted to, for example, +10 degrees, the matching value is fixed, the antenna is deflected -10 degrees and adjusted in such a way that it is again matched (method II). A $\neq$ 10 degree angle results because, to begin with, the center of radiation is not on the connecting line point of rotation-center of radiation of the auxiliary antenna. By means of this test we can determine how much the antenna must still be moved in order to obtain approximately the same angle on both sides. The arrangement of the assembly allows an additional deflection of the antenna by several degrees. The remaining deflection should not exceed one degree, if possible.

10. After these preparations are made, the real measurements can begin. The fastest testing method is as follows: adjust the test antenna to an angle of $+\psi$, fix the matching position, deflect the test antenna to the other side, and note the $-\psi_2$ angle, with which matching is again accomplished. Repeat this process with various angles. It is suggested that the largest possible angle and angle differences be used, e.g., 10, 15, and 20 degrees, as far as the radiation diagram permits. That is, with these angles, to begin with, there are no phase changes with which to contend, and secondly the sensitivity of the measurement is still high enough, on the basis of the diagram. Naturally, a complete diagram $d(\psi)$ may be taken into consideration, only care must be taken that during this relatively long period (and considering several such diagrams) the temperature does not change too much (long-duration stability).

11. The evaluation of the test values is best accomplished by presenting the results of $\varphi(\psi)$ as shown in Diagram 7 and estimating the most probable value. In addition, an evaluation of method III can be conducted, i.e., determination of c (see, for example, Table 9.3 in connection with the adjoining text), which produces the most relatively fast and fairly certain results. The measurements are to be made very carefully, especially the ψ measurements, because these errors have the greatest influence on the overall error. The measurements are to be repeated as controls for various intervals of points of rotation aperture planes.

12. It seems practical to control the temperature on sunny days and to recheck the test position in about one hour in respect to the function of temperature. Great cable position changes are to be avoided during the test. The pieces of cable that are moved on the test antenna and on the sonde connections are to be placed in such a way that they have the largest possible bend radius. All the other cables are to be so placed that they will not be moved too much by the wind. Cable connections are especially to be kept free of tension and other loads (bending). The mechanical stability of the currently available installation (test antenna assembly arrangements) is not adequate in a strong wind. It is, therefore, important that the quietest possible days be selected for the tests.

11. Summary.

All sources of error which may appear in connection with phase measurements are reviewed in detail and discussed in the light of test results. It was shown how, by an exact error analysis, we can work up the most probable test result to a few pars per mille. The construction of the phase testing station is discussed and, at the end, detailed instructions are given in summary.

12. Bibliography,

1. Karl Bauer, "Das Phasenzentrum von Aperturstrahlern" (The Phase Center of Aperture Emitters), AMO (?), Volume 9, 1955, Issue 12, pages 541-546.

2. C. S. Ajoka, "A Microwave Phase Center Plotter," Proceedings IRE, September 1955, page 1088.

3. S. Silver, Microwave Antenna Theory and Design, Rad. Lab. Ser., McGraw-Hill Book Co., New York, Toronto, London, 1949, page 564 ff.

3a. Same, page 587.

4.

4. H. Zuhrt, Elektromagnetische Strahlungsfelder (Electromagnetic Radiation Fields), Springer Verlag (Publishing House), 1953, page 357.